Wake Vortices in Convective Boundary Layer and Their Influence on Following Aircraft

Frank Holzäpfel,* Thomas Gerz,* Michael Frech,† and Andreas Dörnbrack†
DLR, German Aerospace Research Center, D-82234 Weßling, Germany

The decay of three wake vortex pairs of a B-747 aircraft in an evolving and convectively driven atmospheric boundary layer is investigated by means of large-eddy simulations (LES). Convective boundary layers are considered hazardous because the updraft velocities of a thermal may compensate the induced descent speed of the vortex pair such that the vortices stall in the flight path. The LES results illustrate that 1) the primary rectilinear vortices are rapidly deformed on the scale of alternating updraft and downdraft regions; 2) parts of the vortices stay on flight level but are quickly eroded by the turbulence of the updraft; 3) the longest living sections of the vortices are found in regions of relatively calm downward flow, which augments their descent. Strip theory calculations are used to illustrate the temporal and spatial development of lift and rolling moments experienced by a following medium weight class B-737 aircraft. Characteristics of the respective distributions are analyzed. Initially, the maximum rolling moments slightly exceed the available roll control of the B-737. After 60 s the probability of rolling moments exceeding 50% of the roll control has decreased to 0.009% in a safety corridor around the glide path.

Nomenclature

b	= aircraft span
b_0	= initial vortex spacing
c	= section chord
c_l	= section lift coefficient
dP	= probability difference
g	= gravitational acceleration
k	= wave number
L	= lift
L_x, L_y, L_z	= domain size in different directions
L_0	= neutral lift
M	= rolling moment
M_c	= available roll control
m	= aircraft mass
P	= probability
r	= radial coordinate
r_c	= initial core radius
S	= one-dimensional power density spectrum
T_*	= free convection temperature scale
t	= time
u	= axial velocity
u_∞	= flight speed
v	= lateral velocity
v_t	= tangential velocity
w	= vertical velocity
w_0	= initial vortex descent speed
w_*	= free convection velocity scale
x	= axial coordinate in flight direction
y	= spanwise coordinate
z	= vertical coordinate
z_i	= inversion height
α	= angle of attack
α_0	= mean angle of attack
Γ_0	= root circulation
λ	= wavelength
λ_2	= measure for coherent vorticity
ρ	= density
$\prime$	= fluctuating quantity

Introduction

AS a response to lift, aircraft create counter-rotating vortices at the wing tips and at the edges of the flaps, the so-called wake vortices. The wake vortices may exert a serious danger on following aircraft. Therefore, separation standards were established that already limit the capacity of many airports.

Naturally, wake vortices descend below the glide path by mutual induction. However, measurements[1,2] and simulations[3,4] indicate that under certain atmospheric conditions wake vortices stop their descent or even rise again. This hazardous situation is of great concern for reduced spacing operations. As a result, the probability of encountering stalled vortices during approach increases considerably. Therefore, the question of vortex aging achieves primary significance.

The question of what type of meteorological phenomena are candidates to cause this hazardous situation was also raised in the context of the further development of the wake vortex warning system of the Frankfurt airport.[5] The system was established to run the closely spaced parallel runways separately at appropriate meteorological conditions. It predicts the propagation and lifespan of wake vortices in a safety box of 80 m height above ground, based on statistical analyses. This particular height of 80 m was chosen because measurements at Frankfurt airport showed that wake vortices in ground effect do not rebound to this level. Pilot associations recently argued that above the safety box the updrafts in a convectively driven atmospheric boundary layer (CBL) may cause wake vortices to stall or even to rise up to the glide slope. In a CBL, the buoyancy-driven thermals form highly energetic updrafts due to the radiative heating of the ground. The updrafts are surrounded by less turbulent downdraft regions.

In this study, large-eddy simulations (LES) of the evolving CBL have been performed that indicate that wake vortices actually may rise in the CBL when the velocity of the updraft exceeds the induced descent speed of the wake vortices. However, at the same time they are strongly deformed by the large-scale velocity field of the CBL and decay quickly due to the large turbulence intensity prevailing in the updrafts of the CBL.‡

To quantify these qualitative results, lift and rolling moments are assessed by means of strip theory. It is assumed that a B-737

aircraft crosses the CBL along various paths and thereby encounters the wake of B-747 aircraft. Lift and rolling moment distributions are first analyzed as averages along the flight path. Averaging takes into account that the large-scale deformation of the wake vortices reduces the impact time of the encountering aircraft. Then, probabilities of local rolling moments are evaluated in terms of probability density distributions and time series of rolling moments based on various selected threshold levels.

To the authors' knowledge, only one previous example of a numerical simulation of wake vortices in a CBL-similar environment exists.[6] There, the prime interest was to study the effect of atmospheric turbulence on vortex decay. Here, an attempt is made to understand how the peculiarities of the CBL structure (alternating thermals and downdrafts) alter the wake-vortex behavior. Furthermore, the resulting complex flowfield data are used for encounter assessments. Rossow and Tinling[7] give a still up-to-date survey of techniques to compute forces and moments exerted by wake vortices on encountering aircrafts. A more recent overview on numerical and experimental research to characterize wake vortex encounters is given in Ref. 8.

Methods

LES Code and Its Initialization

LES is used to simulate the CBL and the evolution of three superimposed vortex pairs. The numerical method is described in detail by Schmidt and Schumann.[9] The numerical scheme integrates the full primitive equations of motion in their nonhydrostatic form, together with the thermodynamic equation, in three dimensions and as a function of time.[9,10] The subgrid-scale fluxes are determined by means of a first-order closure as described by Dörnbrack.[11]

To achieve an appropriate resolution of both the characteristic scales of the CBL and the wake vortices, a domain size of $L_x = L_y = L_z = 512$ m with a grid volume of $\Delta x \times \Delta y \times \Delta z = 8 \times 2 \times 2$ m^3 is chosen. Periodic boundary conditions are employed in the horizontal directions. At the top and bottom of the domain, free-slip and no-slip conditions are prescribed, respectively.

The dry and quiescent atmospheric boundary layer is intitialized with a uniform temperature and superimposed random perturbations. The CBL is driven by a constant vertical heat flux at the lower surface until the growing thermals reach the top of the domain. Although the convective cells are still growing at this stage, the turbulent variances agree well with empirical scaling relations of the stationary CBL.[12] The ongoing evolution of the CBL is neglectable because the convective timescale is about six times larger than the lifespan of the wake vortices. The mean value of the turbulent kinetic energy (TKE) amounts to 0.9 m^2/s^2.

After three convective timescales, three wake vortex pairs are superimposed on the turbulent flowfield at three selected locations of the domain (Fig. 1). The right part of vortex pair 1 is placed on the shoulder of an updraft ($y = 199$ m and $z = 404$ m) to study the effect of lateral gradients of the vertical wind. The left part is situated in a quite homogeneous low-turbulence downdraft area to investigate maximum lifespans. The second vortex pair is superimposed on a region that covers a strong updraft, a moderate downdraft, and a rather calm area ($y = 386$ m and $z = 222$ m) to examine the effects of axially varying conditions. The third vortex pair, placed on a low altitude ($y = 132$ m and $z = 64$ m) allows investigation of ground effects. The three vortex pairs are sufficiently separated from each other such that mutual influences can be neglected.

The wake vortices are initialized as the superposition of two Lamb–Oseen vortices

$$v_t(r) = \frac{\Gamma_0}{2\pi r}\left(1 - \exp\frac{-1.26\,r^2}{r_c^2}\right) \qquad (1)$$

representing a B-747 aircraft with a root circulation of $\Gamma_0 = 565$ m^2/s and a vortex spacing of $b_0 = 47$ m. An unrealistically large vortex core radius of $r_c = 8$ m has to be chosen to resolve the forced vortex region with four grid points. It is known that the wavelength and growth rates of wave instabilities are a function of r_c/b_0 (Refs. 13 and 14) and that the decay rate of wake vortices with larger core radii may be increased.[15] Therefore, another CBL run was performed
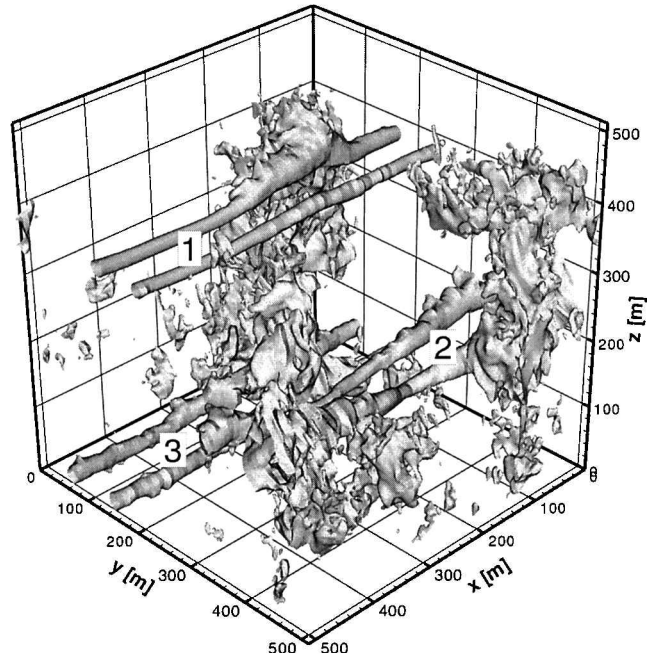

Fig. 1 Isosurfaces of the positive vertical velocity value, $w = 2$ m/s, of the evolving CBL with 10-s-old wake vortices; numbers denote the vortex pairs.

with vortex pair 2, which had an initial core radius of 4 m, resolved by two gridpoints. That run yielded almost identical decay rates compared to the case with $r_c = 8$ m. Another simulation of wake vortices in the CBL with relatively tight vortex cores ($r_c/b_0 = 0.125$) was published[16] that corroborates our current results. Vortex core radii also influence the results of encounter analyses for span ratios of follower to generator $b_f/b_g < 0.5$ (see Ref. 7). Reducing the core radius in our study to $r_c = 4$ m would increase the initial rolling moment experienced by the following B-737 by a factor of 1.4. In piloted simulator investigations[17] of wake vortex encounters, it was found that core radius effects are negligible.

Encounter Analysis

The hazard reduction for aircraft that encounter the deformed and decaying vortex pairs is assessed by strip theory. In strip theory, the load on each wing section is calculated from the local section angle of attack and integrated to estimate the forces and moments exerted on an aircraft for a given velocity field.[18] This straightforward method is chosen because it provides an economic approach to perform the calculations at every one of the more than 4×10^6 grid points. A recent comparison of various simple wake vortex interaction models elucidates the good predictive capabilities of strip theory.[19] A well-known limitation of strip theory is an unreliable load distribution in the vicinity of the vortex cores.[18] For our purpose, the accuracy of strip theory achieved for the overall loading is sufficient to give an insight into the prominent phenomena and to give a realistic estimation of the time span in which the wake vortices alleviate to harmless strengths. Sufficient accuracy is particularly expected for the most interesting final decay of the vortices because then no more intact vortex core structures are observed.[20]

The rolling moment constitutes the most hazardous effect on aircraft that encounter wake vortices coaxially or at small angles.[7] Therefore, this study focuses on the evaluation of rolling moments M, which are normalized by 50% of the available roll control, $M_c = 2.8 \times 10^6$ Nm. The threshold $|M/0.5M_c| = 1$ represents an acceptable value for wake vortex encounters[7] although piloted studies state that the maximum bank angle provides the most appropriate measure for a wake vortex hazard.[17] However, evaluations of the bank angle would have to include aircraft as well as pilot reactions, which is beyond the scope of this study. The current approach resembles, rather, the common arrangement used to study encounter effects in wind-tunnel experiments. There, the following aircraft is mounted fixedly on a traversing mechanism and is equipped with

a force balance or pressure taps on the wings to evaluate loads. To give a more comprehensive view of the forces experienced by the aircraft, the effects of down- and upwashes are also presented in terms of loss and gain of lift $(L - L_0)/L_0$ normalized by neutral lift (weight), $L_0 = m \cdot g$.

As encountering aircraft, the common medium-weight-class B-737 aircraft is chosen; this enables comparisons with flight-test experiments of the NASA Langley Research Center B-737 (Ref. 8). Typical flight conditions prevailing during the early approach are prescribed for the whole domain: The B-737 with a span of $b = 28.4$ m and a weight of 450,000 N flies in clean configuration at a speed of $u_\infty = 150$ m/s in an atmosphere with density $\rho = 1$ kg/m^3.

In the evaluation, the B-737 penetrates the domain in x direction at every (y, z) grid point. Lift L and rolling moment M are integrated according to

$$L = \frac{\rho}{2} u_\infty^2 \int_{-b/2}^{b/2} c(y) c_l[y, \alpha(y)] \, \mathrm{d}y \qquad (2)$$

$$M = \frac{\rho}{2} u_\infty^2 \int_{-b/2}^{b/2} c(y) c_l[y, \alpha(y)] \, y \, \mathrm{d}y \qquad (3)$$

The section lift coefficients c_l are taken from pressure tapping measurements of the DLR-F6 wing–body–engine configuration, which were carried out in the S2MA wind tunnel of ONERA.[21] Eight spanwise $c_l[\alpha(y)]$ sections are interpolated to the 2-m-spaced grid points. The local spanwise section angle of attack is

$$\alpha(y) = w(y)/u_\infty + \alpha_0 \qquad (4)$$

where $\alpha_0 = 0.2$ deg.

Discussion of Results

Convective Boundary Layer

For the purpose of this study, which is to describe the main features of the interaction of the CBL with aircraft wake vortices, the flowfield of the simulated CBL should be as realistic and representative as possible. Therefore, our simulated CBL is compared with data obtained in field and laboratory experiments as well as from other LES.

Figure 1 depicts an isosurface of the positive vertical velocity, $w = 2$ m/s, of the evolving CBL and the three 10-s-old wake vortex pairs in a perspective view. Three convective cells or updraft regions can be identified that are partially merged with the tubular isosurfaces of the upwashes of the trailing vortices. In between the updrafts, a moderate downward flow prevails.

Figure 2 shows normalized velocity and temperature fluctuation patterns along an instrumented aircraft flight path segment and respective simulation data. The data have been collected in evolving CBLs during the European Field Experiment in a Desertification-Threatened Area (EFEDA)[22] at a height of about 50% of the inversion height z_i. The scaling parameters w_* and T_* are taken from free convection scaling.[12] Another data segment would obviously show different curves. Nevertheless, some typical features of a CBL can be well illustrated with this juxtaposition: The updraft velocities exceed the downdraft velocities and distinct small-scale fluctuations are superimposed to the up- and downdraft regions. In the up- and downdraft segments, w' and T' are correlated such that the heat flux $w'T' > 0$. Because of the turbulence, smaller-scale segments exist where w' and T' are anticorrelated $(w'T' < 0)$. The area fraction with a positive heat flux is larger than that of negative heat fluxes.[12]

For the interaction of the CBL and the wake vortices, the TKE of the CBL and its spectral distribution is of particular importance. Figure 3 depicts a one-dimensional TKE spectrum from the LES at $z_i/2$ after three convective timescales and before the wake vortices have been inserted. The range covered by TKE spectra from field measurements is included with crosshatches[12,23]; the spectrum range found in wind tunnel, water tank, and other LES studies[24] is denoted with dots. [The TKE spectra from the literature are calculated according to $k \cdot S_{\mathrm{TKE}}(k)/w_*^2 = 0.5(k \cdot S_{uu}(k)/w_*^2 + k \cdot$
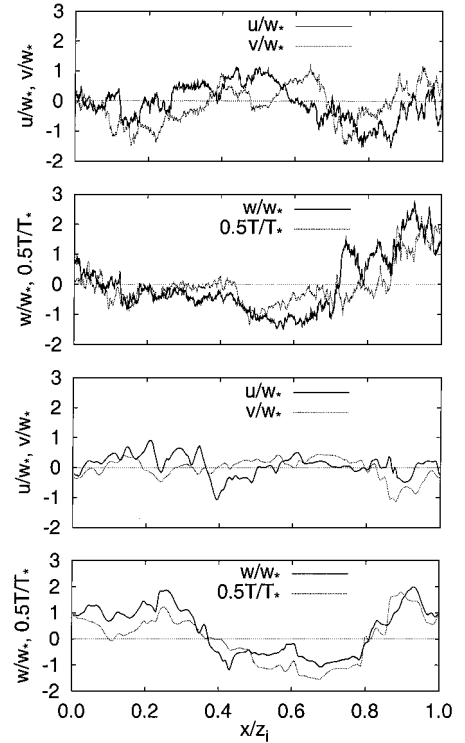

Fig. 2   Normalized velocity and temperature fluctuation patterns along an arbitrary flight path at $z_i/2$; measurement (top) and LES (bottom).
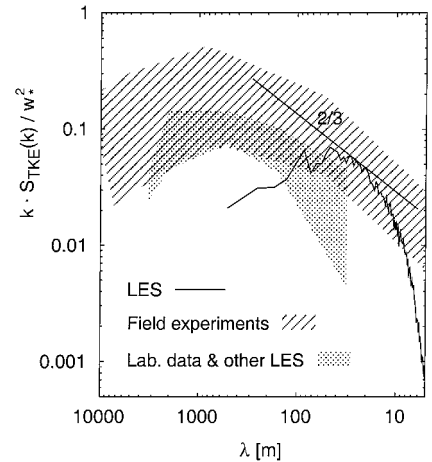

Fig. 3   One-dimensional TKE spectra from the LES at $z_i/2$; range covered by spectra found in field experiments[12,23] indicated with cross hatches; spectra from wind tunnel, water tank, and other LES studies[24] denoted by dots.

$S_{vv}(k)/w_*^2 + k \cdot S_{ww}(k)/w_*^2$. Values for the normalized dissipation rate that are needed to transfer the spectra of field measurements[23] into the current form are taken from Ref. 12, page 164.]

Current computer capabilities do not allow us to simulate sufficiently high effective Reynolds numbers to achieve the wide spectra as observed in field measurements. However, at its most energetic part, the simulated spectrum lies in the range of the field–measured data. Only the largest and smallest scales carry less energy than observed. This reflects that the current CBL is still evolving (energy maximum at smaller scales) and that the LES suffers from too strong effective (turbulent) viscosity at the smallest scales. However, in the wavelength range of 10–100 m of the CBL, which is certainly most sensitive for the interaction with the wake vortices and their turbulent decay,[20] the LES comprises quite well the energy levels of real atmospheric CBLs. The underestimation of energy at smallest scales (below 10 m) extenuates the direct impact of CBL turbulence on the vortex cores; the underestimation of energy at

the scales above 100 m reduces the excitation of Crow-unstable modes.[13] Hence, both effects provide conservative bounds for all results discussed thereafter.

Wake Vortex Behavior

To illustrate the wake vortices graphically, the second eigenvalue λ_2 of the symmetric tensor $S^2 + \Omega^2$ is calculated, which is a measure of the coherent vortex structures.[25] S and Ω are the symmetric and antisymmetric components of the velocity gradient tensor ∇u. Figure 4 shows surfaces of $\lambda_2 = -0.5/s^2$ at $t = 10$ and 40 s. The (arbitrary) temperature isosurface elucidates the fine-scale structure of the surface plumes. Already, at the early stage of $t = 10$ s, the wake vortices are deformed according to their position relative to the up- and downdrafts. At 40 s, the vortices are partially destroyed due to turbulent erosion, especially in the updraft regions. Noticable height differences can be observed for the vortices of pair 1, which was placed on the shoulder of the thermals. The resulting situation of almost solitary vortices may be more dangerous because a solitary vortex decays relatively slowly[26] because the mutually in-
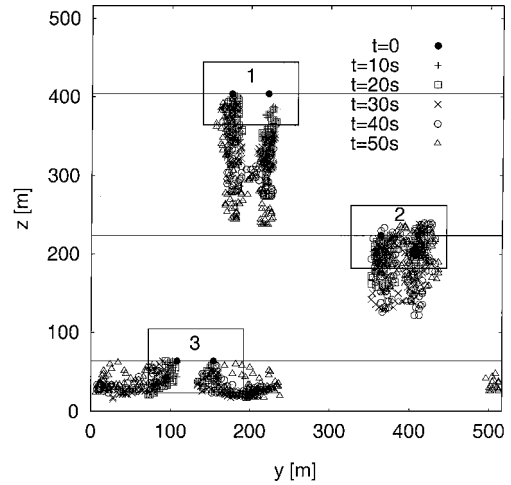
Fig. 5 Evolution of vortex positions seen in flight direction; rectangles surrounding the initial height of vortex pairs denote safety corridors.

duced destruction mechanisms (shortwave and longwave instability, stretching of external turbulent eddies) are less effective.[4,15] The vortex pair in ground effect is moving laterally (compare Fig. 5) and thereby displaces the small-scale surface layer plumes. At $t = 70$ s, all coherent vortices are essentially destroyed.[§]

Figure 5 depicts the evolution of the vortex positions as seen in flight direction for the time span in which they can be uniquely determined by searching local λ_2 minima. The initial vortex heights are denoted by horizontal lines. Because of the different vertical velocities in updrafts and downdrafts, the vortices out of ground effect are mainly stretched in the vertical direction. Maximum height differences of 150 m are estimated. The descent speed varies between -0.4 and 1.8 times the initial descent speed $w_0 = -1.9$ m/s. Some vortex segments of the pairs 1 and 2 actually remain on or even rise up to 20 m above the flight level. In regions with moderate spanwise gradients of w, vortex tilting leads to an increased lateral scatter of vortex positions (pair 2). The vortex pair 3 in ground effect is considerably stretched along typical trajectories of separation and rebound. Some parts even return to their initial position after 50 s.

Encounter Analysis

In this section, lift deviations and rolling moments that are exerted by the vortices and the CBL on a B-737 aircraft are discussed. These are averaged along each flight path to condense the three-dimensional data to two-dimensional plots. The averaging is performed primarily because it takes into account that the large-scale deformation of the vortices reduces the impact time of forces and moments. On the other hand, averaging includes the drawback that contributions of opposite sign may compensate for each other, which will result in an underestimation of the disturbances. Therefore, probabilities of local rolling moments will also be analyzed subsequently.

Figures 6a and 6b display the averaged and normalized lift deviations $(L - L_0)/L_0$ at $t = 0$ and 40 s, respectively. These lift deviations can be interpreted as vertical accelerations of the following B-737 aircraft normalized by the gravitational acceleration. At $t = 0$, the concentric areas with negative accelerations are significantly larger and of about twice the intensity (almost -1 g) of the adjacent areas with positive accelerations. Later, at $t = 40$ s, the areas with lift deviations out of ground effect are mainly stretched in the vertical direction in a similar way to the vortex positions (see Fig. 5). The maximum negative acceleration at $t = 40$ s of $L/L_0 - 1 = -0.52$ is caused by the vortex pair 1 close to $z = 300$ m. This is due to several effects: A large part of these vortices is situated in a homogeneous downdraft of the CBL, where lower turbulence intensities leave the
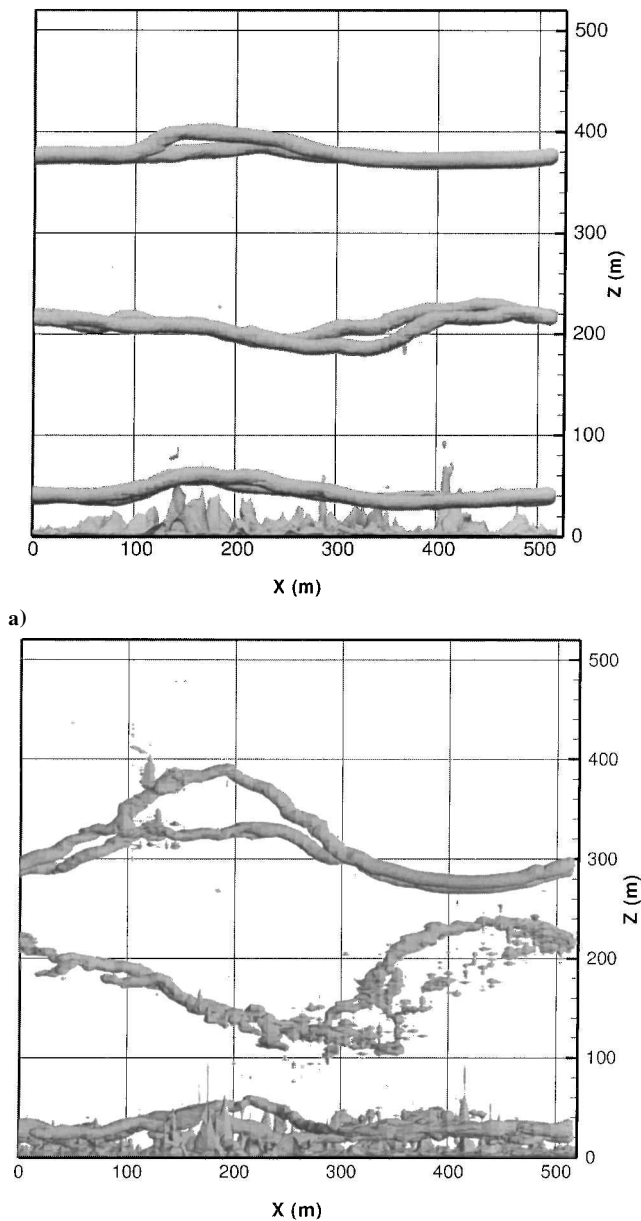

a)

b)

Fig. 4 Side view of $\lambda_2 = -0.5/s^2$ (for definition see text) of the three vortex pairs and an arbitrary temperature isosurface at a) $t = 10$ s and b) $t = 40$ s.
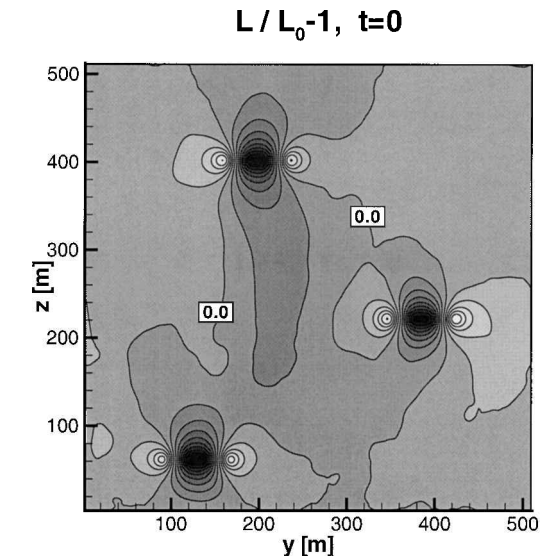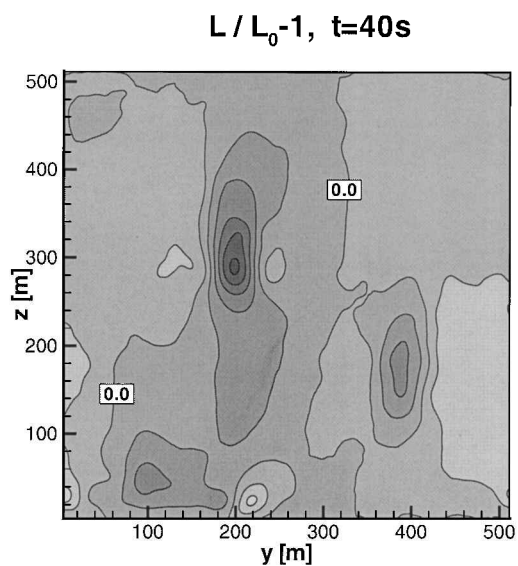

[§]A comprehensive view on the wake evolution can be gained from the animated simulation results, which may be found at http://www.pa.op.dlr.de/wirbelschleppe/conv.html [cited 20 October 2000].

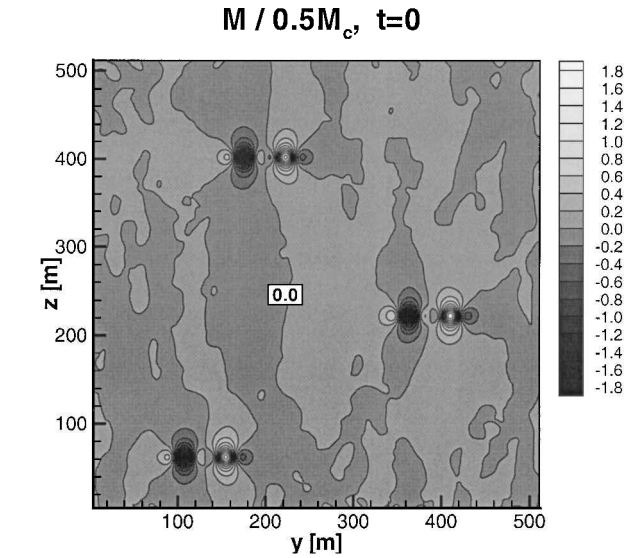## L / L$_0$-1, t=0
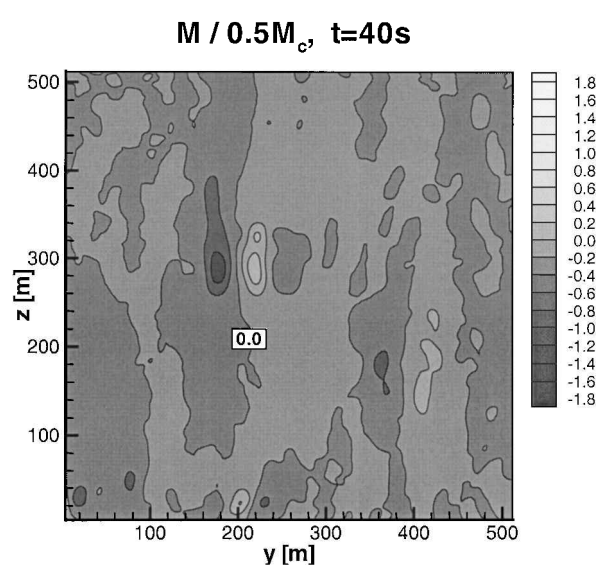

a)

L / L$_0$-1, t=40s

b)

Fig. 6 Mean lift deviations, $L - L_0$, normalized by neutral lift, $L_0 = m \cdot g$, experienced by B-737 aircraft crossing the domain in x direction at every (y, z) position at a) $t = 0$ s and b) $t = 40$ s.

M / 0.5M$_c$, t=0

a)

M / 0.5M$_c$, t=40s

b)

Fig. 7 Mean rolling moment distribution normalized by 50% of available roll control M_c at a) $t = 0$ s and b) $t = 40$ s; $|M \triangleleft 0.5 M_c| = 1$ is used as a threshold level for acceptable encounters.

vortices quite intact. Furthermore, the descent speed in this area of the CBL augments the downwash experienced by the B-737. Finally, the vortices have approached each other, which also intensifies the downwash. At $t = 60$ s only vortex pair 1 still causes accelerations of up to -0.36, and at $t = 80$ s, a maximum value of -0.26 is found. However, these accelerations occur at vertical positions of 180 and 250 m below the glide path, respectively.

The rolling moments at $t = 0$ (Fig. 7a) reach almost the full roll control capability of the B-737, that is, $|M / 0.5 M_c| = 2$, in the vortex centers. The rolling moment signature of one vortex pair consists of two strong primary and four relatively weak counter-rotating secondary areas. Along a horizontal line through the vortex centers, the rolling moments change their sign five times. These multiple sign changes are also found in wind-tunnel experiments.[27] The magnitude and sign of the resulting rolling moment that acts on the encountering aircraft depend on its wing span and its position relative to the vortex pair: The outer secondary areas emerge when only one wing is placed into the updraft of a vortex. The central alternating moments act on the wings when the aircraft has a span smaller than the vortex spacing and is flying in line with the preceding aircraft. It is then solely exposed to the downwash region of the predecessor's wake.

Because of the large-scale deformation of the vortices, the secondary maxima of the moments have already disappeared at $t = 20$ s. As for the lift distribution, the areas of increased rolling moments are stretched vertically, and the lower part of pair 1 maintains the highest moments, which are reduced to a maximum of 0.53 at $t = 40$ s (Fig. 7b). At $t = 60$ s, only the part of pair 1 that is situated in the downdraft area of the CBL can still be identified in a small zone with $|M / 0.5 M_c| < 0.34$. This elucidates that wake vortices in the rather calm downdraft areas are intact for longer time spans. However, far below the glide path, they are a little hazardous.

The probability density distributions (PDD) of nonaveraged rolling moments $(M / 0.5 M_c)$ are delineated in Fig. 8a for the CBL with and without wake vortices. In this presentation, the shapes of the PDDs are almost identical. The narrow-banded curves suggest two interpretations: First, the probability of experiencing high rolling moments is small because of the small volumes occupied by wake vortices. Second, the thermals in the CBL itself exert enhanced rolling moments. We found local maxima of about $M = \pm 0.3 M_c$ in our simulation, that define the background level to which the wake-induced rolling moments will decay asymptotically. Indeed, the forces and moments exerted by individual thermals can be enormous. For example, vertical gust velocities of up to 11.4 m/s
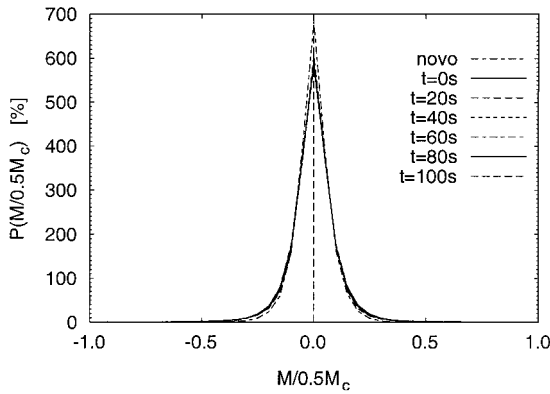
Fig. 8a   Probability density distributions of normalized rolling moments without (labeled as novo) and with wake vortices.
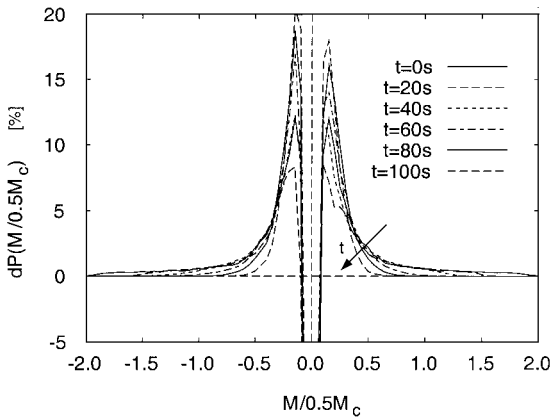

Fig. 8b   Difference of the probability density distributions of normalized rolling moments with and without wake vortices; arrow indicates the temporal sequence of the curves.

associated with a vertical acceleration of 1.42 g were reported by a research aircraft flying at low altitudes over the boreal forest.[28]

To elaborate the rolling moment effects of the wake vortices compared to the CBL, the differences of the respective PDDs are shown in Fig. 8b. The central negative probability differences with values of from -104 to -74% (not shown in Fig. 8b) indicate that the superposition of wake vortices reduces the probability of very small rolling moments. The most probable moments caused by the wake vortices in the simulated CBL amount to $0.15 M_c/2$. Maximum values of $|M/0.5M_c|$ with probabilities of the order of $10^{-5}\%$ decrease from 2.25 at $t = 0$ s to 0.8 at $t = 100$ s. In the further simulation, with core radii of 4 m instead of 8 m, $|M/0.5M_c| \leq 2.97$ and 0.98 at the respective times are obtained.

Figure 9a depicts the probability of finding rolling moments exceeding threshold levels of $|M/0.5M_c| = 1$ and 0.5 in the entire computational domain for initial wake–vortex radii of 8 and 4 m. The threshold level of 0.5 is appropriate to separate wake–vortex induced and CBL induced rolling moments. $P(|M/0.5M_c|) > 0.5$ decreases slightly until $t = 40$ s from 1.6 to 1.2% (as long as the vortex structures are intact) and reaches the probability of 0.06% at $t = 100$ s. Hazardous normalized rolling moments above one are likely to occur with an initial probability of 0.6%. Then the probabilities decrease almost linearly for about 30 s. After 60 s, the probability of hazardous rolling moments has decreased to almost 1% of the initial probability. Note that the probabilities decrease more than two orders of magnitude from 40 to 70 s. This implies that the treatment of encounter by more sophisticated methods is expected to give minor differences in results compared to the simple strip theory. Moreover, even different choices of acceptable threshold levels or encounter probabilities lead to minor time shifts only. Figure 9a further elucidates that the simulation of vortex pair 2 with an initial core radius of 4 m yields almost identical results. (To enable the comparison of simulations with one and three vortex pairs
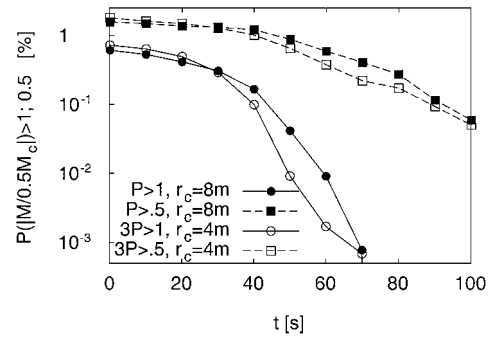

Fig. 9a   Frequency of occurrence of normalized rolling moments greater than 1, respectively, 0.5; results of simulations with initial core radii of $r_c = 8$ and 4 m.
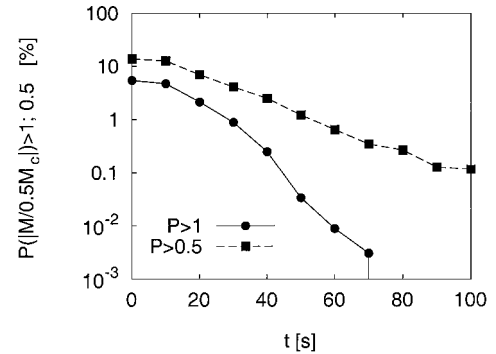

Fig. 9b   Frequency of occurrence of normalized rolling moments greater than 1, respectively, 0.5 in the three saftey corridors, $r_c = 8$ m.

the probability of rolling moments in the single vortex-pair data had to be multiplied by three.)

Flight-corridor specific probabilities of critical encounters are achieved by evaluating the flight track of the follower aircraft in a safety window around the glide path. The size of the window is determined by the accuracy with which aircraft can follow the nominal glide path of the instrument landing system (ILS). At Frankfurt airport a study yielded approximate lateral and vertical standard deviations of 30 and 20 m, respectively, at a distance of 10 mile from the threshold for over 36,000 aircraft approaches, (private communication with M. Maiss, DFS Deutsche Flugsicherung, Offenbach, Germany, May 2000). The accuracy increases with decreasing distance to the runway. Given a safety corridor that extends over two standard deviations in all four directions from the nominal glide path (a window width of 120×80 m², see Fig. 5), Fig. 9b shows that the initial probability of encountering a critical rolling moment ($|M/0.5M_c| = 1$) amounts to 5.4%. At $t = 60$ s, which corresponds to minimum radar separation of 2.5 n mile when assuming a flight velocity of 75 m/s, the probability has decreased to 0.009%.

At $t = 60$ s probabilities of rolling moments almost coincide in the safety corridor and in the whole simulation domain. This reveals and confirms our earlier finding that at about 1 min after the virtual passage of the wake–vortex producing B-747, the simulated rolling moments experienced by the wake encountering B-737 are mainly due to the natural turbulence of the CBL to which the wake-induced rolling moments have decayed in the meantime.

Conclusions

The accelerated decay of aircraft wake vortices in a convectively driven and evolving atmospheric boundary layer was investigated by means of LES. The main challenge was the appropriate representation of the CBL on one side and the wake vortices on the other because the respective characteristic length scales differ by a factor of about 1000. A compromise between the two scale regimes was found by choosing a relatively small domain size that allowed us to study an evolving CBL where typical turbulence and velocity distributions prevail at inversion heights below 500 m. On the other

hand, the wake vortices were modeled with relatively large initial core radii to account for their proper resolution. With an additional simulation it could be shown that vortex cores with 50% smaller radii do not change the rolling moments of an encountering aircraft and the respective probabilities significantly.

The LES elucidate that the wake vortices are rapidly deformed at scales of the alternating updraft and downdraft regions. It is shown that segments of the wake vortices can stall at flight level but that they are quickly eroded by the turbulent updrafts at the same time. The longest living sections of the vortices are found in regions of relatively calm downdraft flow that augments their descent.

The current investigation treats exactly the situation where the strength of the updrafts just compensates the self-induced descent speed of the wake vortices. This allows extension of the conclusions to CBL cases with stronger and weaker thermals: In the weaker CBL case, the common situation prevails where wake vortices descend below the glide path. In a stronger CBL, pieces of the wake may even rise considerably above flight level, but the turbulence level is also increased in the updrafts, which further augments the decay rate of those vortex pieces.

Encounter analyses by means of strip theory elucidate that the deformation and decay of the vortex pairs counteract and dominate the potentially hazardous effects of rising wake vortices. In the LES results, the probability of encountering a potentially hazardous rolling moment ($|M/0.5M_c| = 1$) in a saftey corridor has decreased to 0.9% at $t = 30$ s and is reduced to 0.009% after 60 s. At this time, the wake-induced rolling moments have almost decayed to the background level that originates from turbulence in the CBL.

Main differences from the presented results are expected when a following aircraft flies in high-lift configuration at half the speed used in the current study. This would probably double the normalized rolling moments. Furthermore, the large core radii imply an underestimation of the rolling moments by a factor of 1.4 initially. Although both effects are strong in early times after fly-by, they nevertheless, will modify the potentially hazardous timespan behind the B-747 wake–generator aircraft only slightly because the vortex decay is so rapid in a CBL.

Acknowledgments

References

[1]Zak, J. A., and Rodgers, W. G., Jr., "Documentation of Atmospheric Conditions During Observed Rising Aircraft Wakes," NASA CR-4767, 1997.

[2]Greenwood, J. S., and Vaughan, J. M., "Measurements of Aircraft Wake Vortices at Heathrow by Laser Doppler Velocimetry," *Air Traffic Control Quarterly*, Vol. 6, No. 3, 1998, pp. 179–203.

[3]Proctor, F. H., Hinton, D. A., Han, J., Schowalter, D. G., and Lin, Y.-L., "Two Dimensional Wake Vortex Simulations in the Atmosphere: Preliminary Sensitivity Studies," AIAA Paper 97-0056, 1997.

[4]Holzäpfel, F., Gerz, T., and Baumann, R., "The Turbulent Decay of Trailing Vortex Pairs in Stably Stratified Environments," *Aerospace Science and Technology* (to be published); also AIAA Paper 2000-0754, 2000.

[5]Gurke, T., and Lafferton, H., "The Development of the Wake Vortices Warning System for Frankfurt Airport: Theory and Implementation," *Air Traffic Control Quarterly*, Vol. 5, No. 1, 1997, pp. 3–29.

[6]Corjon, A., Darracq, D., Venzac, P., and Bougeault, P., "Three-Dimensional Large Eddy Simulation of Wake Vortices. Comparison with Field Measurements," AIAA Paper 97-2309, 1997.

[7]Rossow, V., and Tinling, B., "Research on Aircraft/Vortex–Wake Interactions to Determine Acceptable Level of Wake Intensity," *Journal of Aircraft*, Vol. 25, No. 6, 1988, pp. 481–492.

[8]Vicroy, D., Brandon, J., Greene, G., Rivers, R., Shah, G., Stewart, E., and Stueuer, R., "Characterizing the Hazard of a Wake Vortex Encounter," AIAA Paper 97-0055, 1997.

[9]Schmidt, H., and Schumann, U., "Coherent Structure of the Convective Boundary Layer Derived from Large-Eddy Simulations," *Journal of Fluid Mechanics*, Vol. 200, 1989, pp. 511–562.

[10]Krettenauer, K., and Schumann, U., "Numerical Simulation of Turbulent Convection over Wavy Terrain," *Journal of Fluid Mechanics*, Vol. 237, 1992, pp. 261–299.

[11]Dörnbrack, A., "Broadening of Convective Cells," *Quarterly Journal of the Royal Meteorological Society*, Vol. 123, No. 540, 1997, pp. 829–847.

[12]Stull, R. B., "An Introduction to Boundary Layer Meteorology," *Atmospheric Sciences Library*, Kluwer Academic, Norwell, MA, 1988, pp. 117–120.

[13]Crow, S. C., "Stability Theory for a Pair of Trailing Vortices," *AIAA Journal*, Vol. 8, No. 12, 1970, pp. 2172–2179.

[14]Leweke, T., and Williamson, C. H. K., "Cooperative Elliptice Instability of a Vortex Pair," *Journal of Fluid Mechanics*, Vol. 360, 1998, pp. 85–119.

[15]Moet, H., Darracq, D., Laporte, F., and Corjon, A., "Investigation of Ambient Turbulence Effects on Vortex Evolution Using LES," AIAA Paper 2000-0756, 2000.

[16]Lin, Y. L., Han, J., Zhang, J., Ding, F., Arya, S. P., and Proctor, F. H., "Large Eddy Simulation of Wake Vortices in the Convective Boundary Layer," AIAA Paper 2000-0753, 2000.

[17]Sammonds, R., and Stinnet, G., Jr., "Criteria Relating Wake Vortex Encounter Hazard to Aircraft Response," *Journal of Aircraft*, Vol. 14, No. 10, 1977, pp. 981–987.

[18]McMillan, O., Schwind, R., Nielsen, J., and Dillenius, M., "Rolling Moments in a Trailing Vortex Flowfield," *Journal of Aircraft*, Vol. 15, No. 5, 1978, pp. 280–286.

[19]de Bruin, A. C., "WAVENC, Wake Vortex Evolution and Wake Vortex Encounter, Publishable Synthesis Report," National Aerospace Lab., NLR-TR-2000-079, Amsterdam, 2000.

[20]Gerz, T., and Holzäpfel, F., "Wingtip Vortices, Turbulence, and the Distribution of Emissions," *AIAA Journal*, Vol. 37, No. 10, 1999, pp. 1270–1276.

[21]Hoheisel, H., and Geisler, P., "Results of DLR-ONERA-Experiments on the DLR-F4/1-Wing-Body-Engine-Configuration," Institut für Entwurfsaerodynamik, DLR-IB 129-91/26, Braunschweig, Germany, 1991.

[22]Michels, B., and Jochum, A., "Heat and Moisture Flux Profiles in a Region with Inhomogeneous Surface Evaporation," *Journal of Hydrology*, Vol. 166, No. 3–4, 1995, pp. 383–407.

[23]Kaimal, J. C., Wyngaard, J. C., Haugen, D. A., Coté, O. R., Izumi, Y., Caughey, S. J., and Readings, C. J., "Turbulence Structure in the Convective Boundary Layer," *Journal of Atmospheric Sciences*, Vol. 33, No. 11, 1976, pp. 2152–2168.

[24]Fedorovich, E., and Kaiser, R., "Wind Tunnel Model Study of Turbulence Regime in the Atmospheric Convective Boundary Layer," *Buoyant Convection in Geophysical Flows, NATO ASI Series, Series C: Mathematical and Physical Sciences*, edited by E. J. Plate, E. E. Fedorovich, D. X. Viegas, and J. C. Wyngaard, Vol. 513, Kluwer Academic, Norwell, MA, 1998, p. 359.

[25]Jeong, J., and Hussain, F., "On the Identification of a Vortex," *Journal of Fluid Mechanics*, Vol. 285, 1995, pp. 69–94.

[26]Sreedhar, M., and Ragab, S., "Large Eddy Simulation of Longitudinal Stationary Vortices," *Physics of Fluids*, Vol. 6, No. 7, 1994, pp. 2501–2514.

[27]Hegen, G., "Wake Encounter Test in DNW Wind Tunnel—Test Number: 98-1116," National Aerospace Lab., NLR-CR-98291, Amsterdam, 1998.

[28]MacPherson, J. I., and Betts, A. K., "Aircraft Encounters with Strong Coherent Vortices over the Boreal Forest," *Journal of Geophysical Research*, Vol. 102, No. D24, 1997, pp. 29,231–29,234.